Exploiting existing ground-based remote sensing networks to improve high-resolution weather forecasts

Article

Published Version

EXPLOITING EXISTING GROUND-BASED REMOTE SENSING NETWORKS TO IMPROVE HIGH-RESOLUTION WEATHER FORECASTS

BY A. J. ILLINGWORTH, D. CIMINI, C. GAFFARD, M. HAEFFELIN, V. LEHMANN, U. LÖHNERT, E. J. O'CONNOR, AND D. RUFFIEUX

Accurate and reliable existing sources of observations in the lower atmosphere that are currently underexploited are proposed for the evaluation and initialization of high-resolution weather forecast models.

The high-resolution (1 km) forecasting models that are now run operationally by many national meteorological and hydrological services promise to provide increasingly accurate high-resolution forecasts of impending hazardous weather, ranging from flash floods to episodes of poor air quality. Satellites can provide data in the upper troposphere; however, if this promise is to be fulfilled, in particular for short-range forecasts, a new generation of high-density observations through the lower few kilometers of the atmosphere, including the boundary layer, is required in real time. First, these observations can be used to check that the parameterization schemes inherent in such models lead to a realistic representation of the atmosphere. If the observations have known uncertainties and any biases with respect to the model can be quantified, then they can be used in near–real time for *data assimilation*, so that the models used for both nowcasting (1–3 h) and for weather forecasting can be initialized with the best possible representation of the current state of the atmosphere.

The World Meteorological Organization (WMO) statement of guidance (WMO 2014) on observations for global numerical weather prediction (NWP) concludes that the four *critical atmospheric variables* that are not adequately measured by current or planned systems are (in order of priority) as follows: 1) wind profiles at all levels, 2) temperature and humidity profiles of adequate vertical resolution in a cloudy area, 3) precipitation, and 4) snow mass. With respect to clouds, the document states, "Surface stations measure cloud cover and cloud bases with a temporal resolution and accuracy that is acceptable but a horizontal resolution that is marginal in some areas and missing over most of the Earth…Active optical (lidar) and microwave (radar) instruments are required to give more information on the 3D distribution of cloud water and ice amounts and cloud-drop size. Some research instruments have been launched and more

are planned" (WMO 2014, p 7). For three-dimensional aerosol distribution, WMO (2014, p. 8) states, "Assimilation of aerosols is generally immature in global NWP but is likely to increase in importance… Lidar measurements will be required to provide vertically resolved information; research demonstrations are under way." Finally, for three-dimensional winds, they conclude the following: "There is currently no present or planned capability. Research is required on indirect observations via sequences of geostationary infrared imagery, or through Doppler enabled microwave sensors" (WMO 2014, p. 9). Two recent documents (NRC 2009, 2010) concluded that the structure and variability of the lower troposphere is currently not well known because vertical profiles of water vapor, temperature, and winds are not systematically observed and that this lack of observations results in the planetary boundary layer being the single most important undersampled part of the atmosphere.

In this paper we report on a recent Cooperation in Science and Technology (COST) action financed by the European Union, European Ground-Based Observations of Essential Variables for Climate and Operational Meteorology (EG-CLIMET). A major constraint is the absence of funding for new networks of new expensive instruments, so the report concentrated on existing instruments. The final report, which is freely available online (Illingworth et al. 2013; COST 2013), identified four ground-based profiling instruments that are currently underexploited and that have the potential to provide profiles of aerosol and cloud backscatter, winds, temperature, and humidity in real time: 1) automatic lidars and ceilometers (ALCs), 2) Doppler lidars, 3) wind profilers, and 4) microwave radiometers. In the following sections, we consider their ability to operate for long periods unattended, their ease of calibration, the accuracy that can be achieved, and provide examples of their potential impact for improving the performance of operational NWP models.

ALCs. *Operational aspects and potential NWP impacts.* Low-power and sensitive ALCs transmit a short pulse of laser radiation, with wavelengths ranging from 355 to 1064 nm, and receive a backscattered signal with a delay that provides range information. The name *ceilometer* suggests they were originally conceived to measure cloud-base altitude, but the sensitivity of current ceilometers and automatic low-power lidars is sufficient to provide profiles of aerosol backscattered power within the boundary layer and potentially into the free troposphere. For simplicity we now refer to these systems collectively as ALCs. Figure 1a shows a typical day's data from an ALC with weak aerosol returns below 1 km, a high return until 0900 UTC just below 2 km from a water cloud that extinguishes the lidar beam, supercooled water clouds at 3–4 km from 0900 to 1200 UTC, and then after 1700 UTC an ice cloud that is partially penetrated by the ALC.

The Cloudnet project (Illingworth et al. 2007) demonstrated that ALCs are reliable instruments requiring minimal maintenance and that they can be used to quantify the properties of clouds for long-term comparisons of observations of clouds with their representation in forecast models. Barrett et al. (2009) used ALC and radar observations to evaluate forecasts of clouds within the boundary layer. Morille et al. (2007) proposed a portable method to retrieve and classify atmospheric layers (i.e., cloud and aerosol layers, the boundary layer). Monitoring of the atmospheric boundary layer diurnal evolution using ALCs is a topic of active research (e.g., Pal et al. 2013; Haeffelin et al. 2012; Emeis et al. 2008; Münkel et al. 2007). ALCs provided direct evidence (Figs. 1b–d) of the height of the ash cloud following the volcanic eruption of April 2010 in Iceland; a network of ALCs has the potential to track the movement of such ash clouds (e.g., Flentje et al. 2010). Figure 2 provides an indication of the number of ALCs currently operated by European weather services; there are also several hundred ALCs operated by other agencies, but these are not plotted in the figure. It should be noted that while the majority of the ALCs shown in Fig. 2 have the capacity to provide backscatter profiles, at this date most European weather services only record

AFFILIATIONS: Illingworth—Department of Meteorology, University of Reading, Reading, United Kingdom; Cimini—IMAA, CNR, Potenza, and CETEMPS, University of L'Aquila, L'Aquila, Italy; Gaffard—Met Office, Reading, United Kingdom; Haeffelin—Institut Pierre Simon Laplace, Ecole Polytechnique, Palaiseau, France; Lehmann— Deutscher Wetterdienst Meteorologisches Observatorium, Lindenberg, Germany; Löhnert—Institute for Geophysics and Meteorology, University of Cologne, Cologne, Germany; O'Connor—Department of Meteorology, University of Reading, Reading, United Kingdom, and Finish Meteorological Institute, Helsinki, Finland; Ruffieux—Meteo-Swiss, Payerne, Switzerland

CORRESPONDING AUTHOR: Anthony J. Illingworth, Department of Meteorology, University of Reading, Earley Gate, P.O. Box 243, Reading RG6 6BB, United Kingdom
E-mail: a.j.illingworth@reading.ac.uk

The abstract for this article can be found in this issue, following the table of contents.
DOI:10.1175/BAMS-D-13-00283.1

In final form 10 February 2015

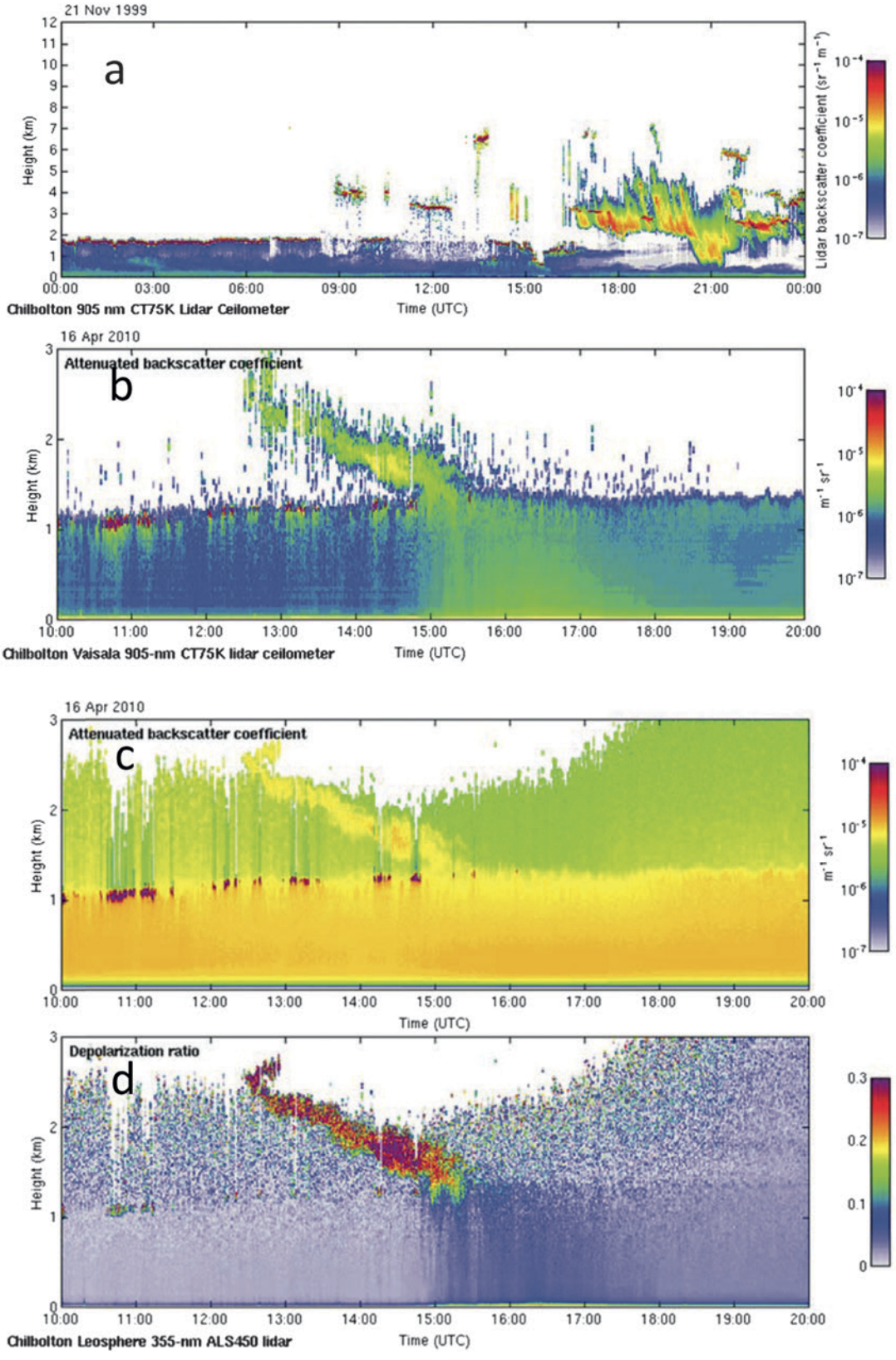

Fig. 1. Examples of ceilometer and lidar profiles: (a) 905-nm ceilometer-attenuated backscatter profile for a 24-h period over Chilbolton, United Kingdom, showing that liquid water clouds, ice clouds, and aerosol in the boundary layer are all detected. (b) Detection of volcanic ash over Chilbolton with ceilometer at 905 nm. (c) As in (b), but at 355 nm. (d) Elevated value of the depolarization ratio at 355 nm clearly identifies the presence of volcanic ash.

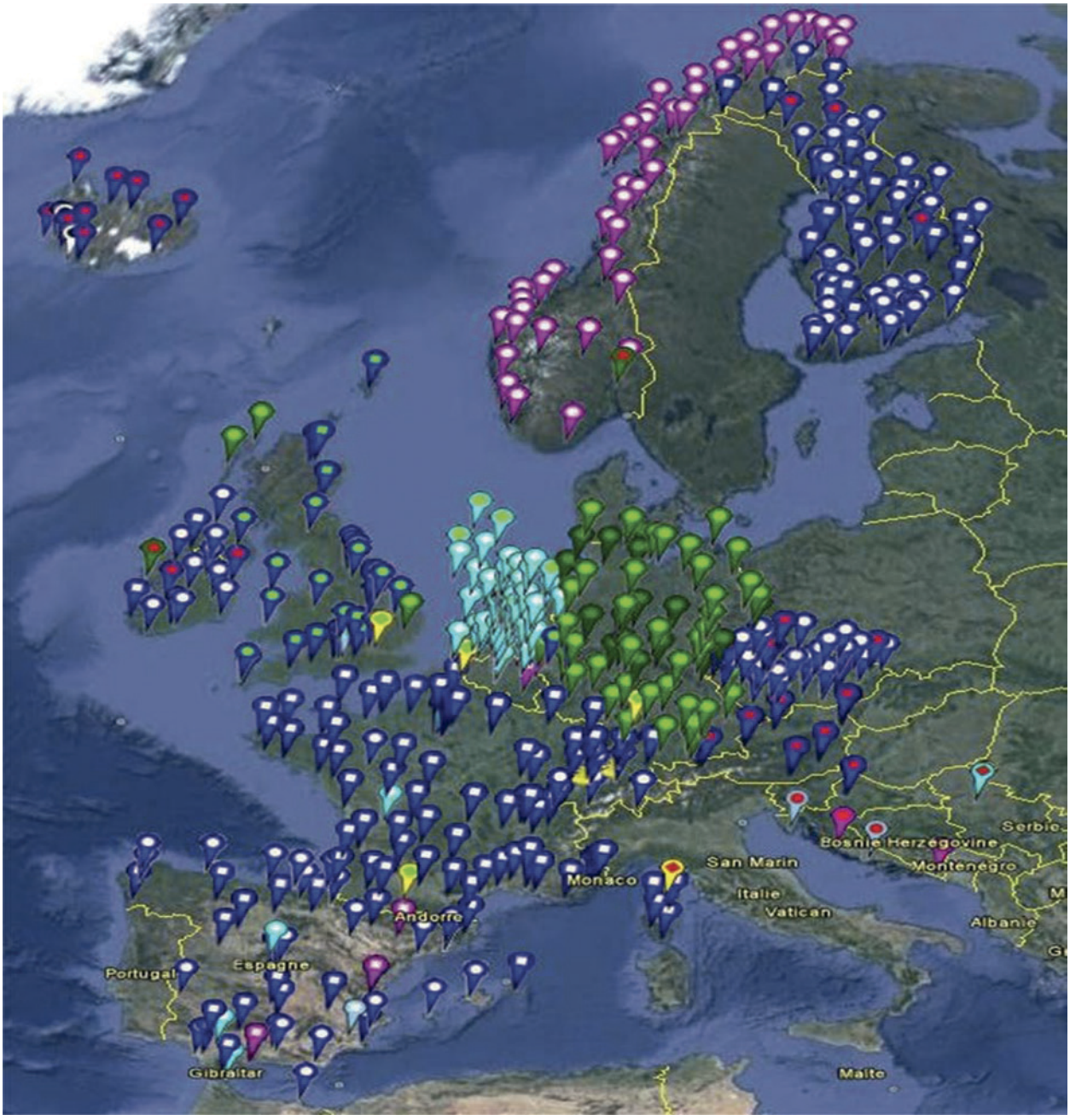

Fig. 2. Ceilometers over Europe operated by national weather services as part of the 5-yr EUMETNET EUCOS E-PROFILE program (www.eumetnet.eu/e-profile) launched in 2013. Goal is to have the ceilometers networked to provide backscatter profiles in near–real time. Symbols comprise a colored arrow with a square, circle, or diamond symbol at the top. Instrument type is designated by the color of the arrow and the shape of the symbol: Vaisala CT25K (dark blue circle), Vaisala CL31K (dark blue square), Vaisala CL51K (dark blue diamond), Eliasson CBME80 (purple circle), Jenoptik CHM15k (green circle), Vaisala CT12 (light blue circle), research lidars (yellow circle), and unknown (white circle). Color of the symbol refers to availability of data: green is for stations storing raw ALC profiles and providing links to quick-look images; red is for stations storing data without providing quick-look images; and white is for stations that do not store ALC data. Colors refer to different ceilometer models. [Courtesy of W. Thomas, Deutscher Wetterdienst (DWD)]

cloud-base heights. Figure 3 shows an example comparison of the observed ALC backscatter from clouds with the backscatter predicted by the Met Office forecast model. More of these observation-minus-background ($O - B$) model statistics are planned to establish the magnitude of any biases in the observations or the model. If this can be achieved, then tests with assimilating the data can be carried out.

The vertical range of an ALC typically extends to between 7.5 and 15 km from the surface, but it should be noted that the lidar signal is severely attenuated by liquid water clouds, so that profiles can only be obtained up to cloud base (and about 200 m into such clouds). Low-level liquid water clouds are most frequent in winter and in northern Europe. The native vertical resolution can be as low as 1.5 m with 5-s temporal resolution, but to increase sensitivity, the raw data are usually integrated up to 15–30 m in the vertical and 15–60 s in time. The minimum range can be lower than 100 m or as high as 1 km, depending on the optical arrangement and the overlap resulting from the physical separation of the receiver and transmitter. Correction of the signal is possible for part of the overlap region. Stray background light (solar radiation) entering the detector chain leads to a drop in sensitivity during the day.

Calibration and accuracy. The instrument records a signal that is proportional to the attenuated backscatter coefficient. To obtain a profile of the attenuated backscatter coefficient (m^{-1} sr^{-1}), the instrument calibration coefficient must be derived. An extinction profile can be derived from the attenuated backscatter coefficient using the lidar equation (e.g., Klett 1981), provided the extinction-to-backscatter ratio (sr) is known. This ratio is commonly named "lidar ratio" S. The value of S in water clouds is well known, but it is variable in ice clouds and for aerosols. This introduces an error in the derived extinction of about a factor of 2. The ALC can also be used to measure the solar background light; with knowledge of the solar zenith angle, this can be converted into a cloud optical depth.

Some ALCs emit polarized pulses and detect the return in both the copolar (same polarization as emitted) and the cross-polar channel. The ratio of the cross-polar return to the copolar return is reported as the depolarization ratio, and it gives an indication

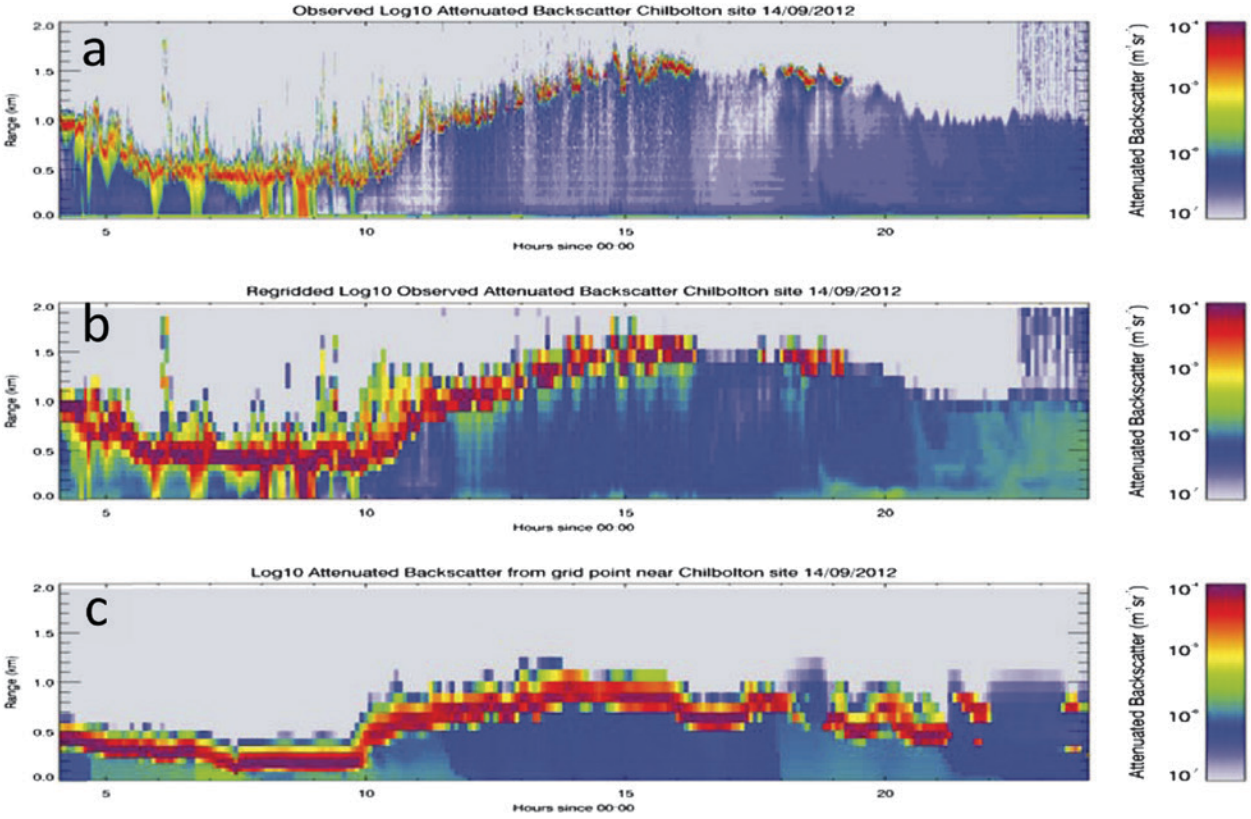

Fig. 3. Cloud representation in NWP models. (a) Observed attenuated backscatter coefficient from Chilbolton for a 24-h period. (b) Observations averaged to the NWP model vertical grid. (c) Backscatter profile predicted by the Met Office 1.5-km-resolution forecast model, showing that the breakup of the low-level water cloud is well captured by the model. [Figure courtesy of Owen Cox and Cristina Charlton-Perez, Met Office.]

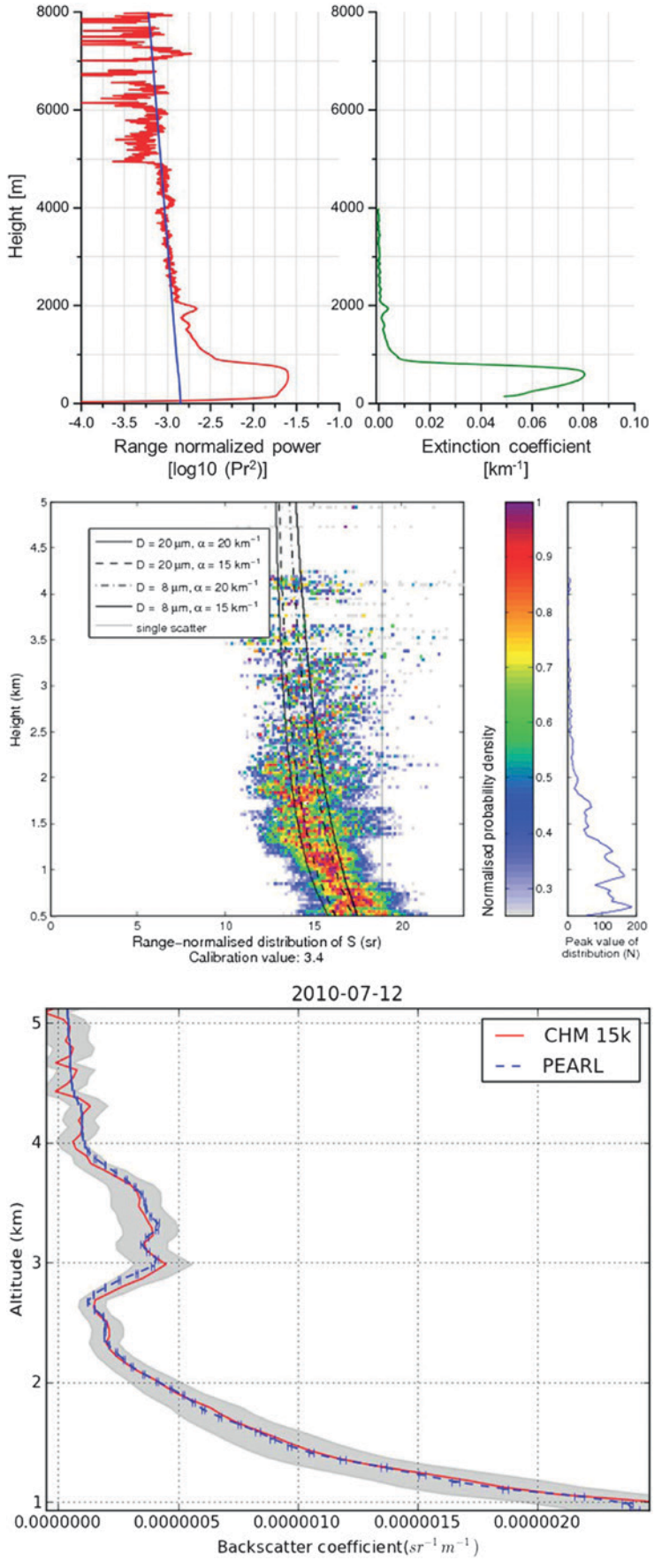

of the shape of the particles responsible for the backscatter. Spherical particles (such as cloud droplets and hygroscopic aerosol at high relative humidities) have a very low depolarization ratio, whereas dry desert dust, volcanic ash (see Fig. 1d), and ice particles have a much higher depolarization ratio. To avoid the large returns due to specular reflection from aligned pristine ice crystals, ALCs are generally pointed 3°–5° off zenith.

Figure 4 describes how calibration is possible using naturally occurring targets: the known molecular backscatter in aerosol-free regions, aerosols observed simultaneously with a sun photometer instrument (Wiegner and Geiß 2012), and liquid clouds that extinguish the signal (O'Connor et al. 2004). As a result the performance of each instrument can

Fig. 4. (top) Automatic lidar and ceilometer calibration techniques. (left) Use of the near-infrared molecular attenuated backscatter at 3–4-km height integrated for 2 h (signal in red, theoretical attenuated molecular profile in blue). The observed profile has been scaled to match the known attenuated molecular profile. (right) The extinction profile (green) scaled so that it matches the integrated aerosol optical depth derived from a collocated sun photometer. (middle) Calibration technique for the water cloud extinction method, relying on the integrated attenuated backscatter return for single scattering being equal to the reciprocal of twice the liquid ratio S. The dotted line is the theoretical value of S = 18.8 ± 1 sr for cloud water droplets at 910 nm. For most ceilometers a range-dependent correction for multiple scattering must be applied (solid and dashed lines). In this example the factory calibration has been adjusted by a factor of 3.4, so that the value of S derived from observed integrated backscatter return over one month agrees with the theoretical predictions. Also shown is the number of individual profiles containing suitable liquid clouds used for the calibration as a function of the height of the cloud. (bottom) Independent evaluation of the molecular calibration technique for a Jenoptik CHM15K ceilometer operating at 1064 nm by comparison with a collocated lidar system having a much more powerful laser at the same wavelength.

be monitored remotely and any malfunction can be rapidly identified. The sensitivity of ALCs depends on the emitted power, telescope design, averaging time, background light, and the strength of the backscattered return from atmospheric targets. Daytime conditions are a much harsher test than nighttime because of the influence of the solar background as a noise source. Figure 5 shows the comparative sensitivity achieved by various ALCs during the day by estimating the minimum detectable backscatter signal that is significantly higher than the background noise. For comparison purposes the sensitivity is calculated for an integration of 30 s; longer integrations would lead to the same increase in sensitivity for all instruments. In Fig. 5, the minimum detectable attenuated backscatter as a function of height has been expressed in terms of extinction (m^{-1}) assuming a lidar ratio of 16 sr; this value has been selected as typical for liquid water clouds and is the median value for the range (2–50 sr) observed in ice clouds and aerosol. A smaller extinction coefficient indicates a more sensitive instrument. The curves in Fig. 5 indicate that the sensitivity of different ALCs can vary over two orders of magnitude.

DOPPLER LIDARS. *Operational aspects and potential NWP applications.* In contrast to ceilometers that have been in use for many years, Doppler lidars are a recent development. These portable autonomous systems have been developed using new solid-state fiber-optic technology. The first were deployed less than a decade ago; consequently, there are no established networks and the use of Doppler lidar data in NWP is in its infancy. Studies during the COST action have established that they have the ability to continuously monitor the wind vector throughout the boundary layer using the return from aerosol particles and that the instruments can operate unmanned with minimal maintenance. Doppler lidars are insensitive to daylight because of the wavelength used, but, as for other lidars, the signal is attenuated by liquid clouds. Two implementations are available for these robust and low-powered systems: pulsed and continuous wave (CW), both using the time delay to provide the range information. Minimum range is typically 50–90 m, with the maximum range varying from 2 to 10 km. Pulsed systems use the delay time to provide the range information, whereas CW systems adjust the focus of the telescope to provide the range information; hence, these are most suitable for close range operation, typically from 10 to 300 m. Both implementations require averaging to achieve the required sensitivity.

Figure 6 describes how, when operated at vertical incidence, the backscatter signal and its Doppler shift can provide an unambiguous estimate of the height of the mixing layer, the turbulent dissipation energy rates, and the origin of the daytime and nighttime

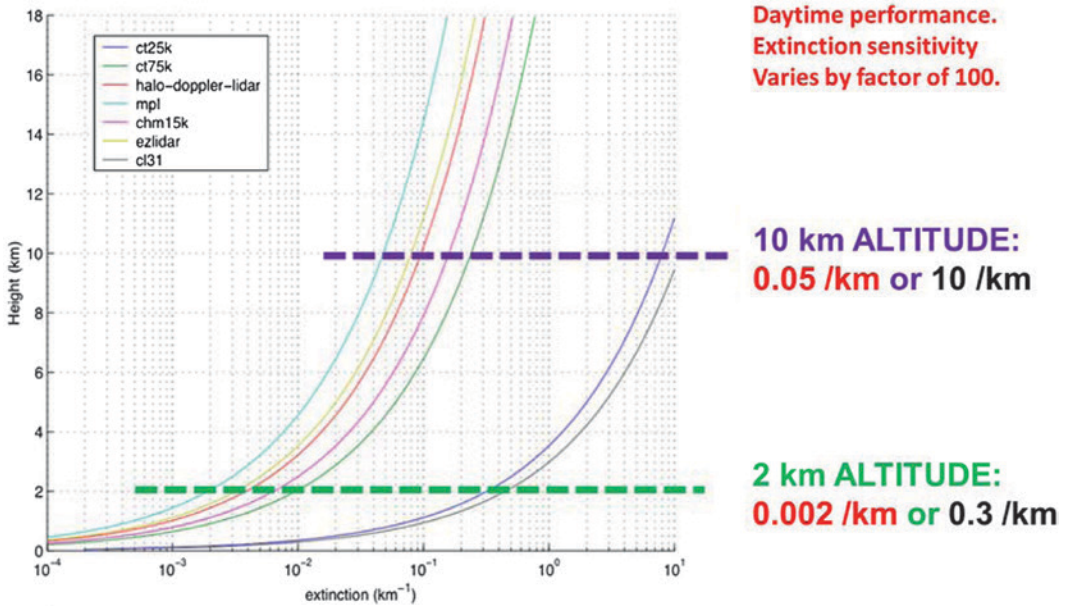

Fig. 5. Daytime sensitivity to ice clouds for various ceilometer systems as a function of altitude showing changes of two orders of magnitude for the different instruments; a smaller extinction coefficient indicates a more sensitive instrument. Extinction is the parameter needed by modelers, and it has been derived from the backscatter sensitivity, assuming a lidar ratio of 16 (see text).

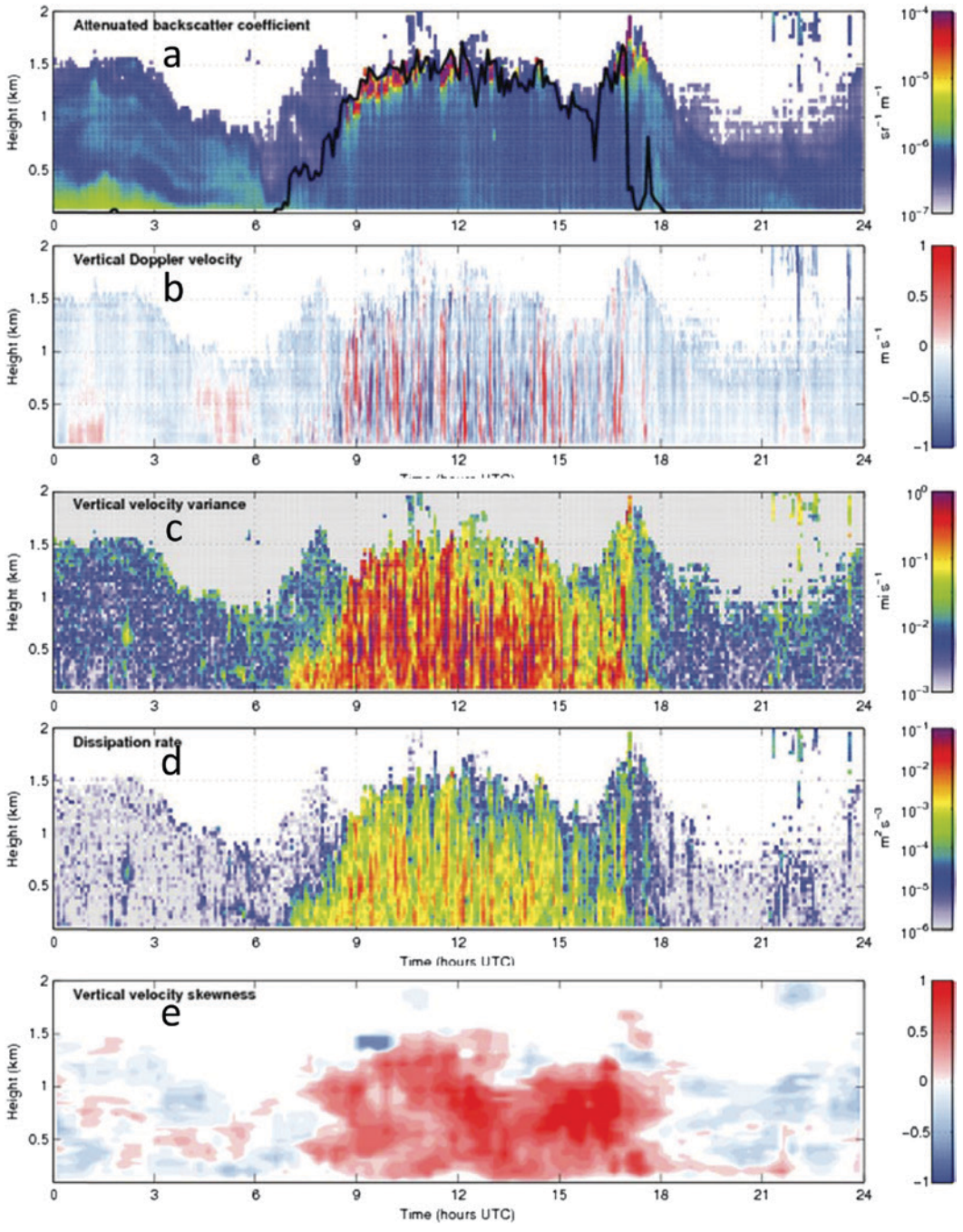

Fig. 6. Doppler lidar products. Aerosol particles act as reliable tracers of the air motion. When operated at vertical incidence, Doppler lidars operating at near-infrared (IR) wavelengths exploit the return from aerosol particles to detect convective motions and the evolution of the mixing height. (a)–(e) Observations from a Halo Photonics system taken at a rural site (Chilbolton) over a 24-h period. (a) Attenuated backscatter coefficient. The black line is the mixing-level height (the top of the region of the boundary layer in constant contact with the surface) derived from the (b) Doppler velocities and specifically from the sharp gradient in the (c) vertical velocity variance. (d) Turbulent energy dissipation rate. The vertical velocity fluctuations can be used to estimate turbulent dissipation energy rates (e.g. O'Connor et al. 2010). The dissipation rate varies over several orders of magnitude, and the delineation between the turbulent convective daytime boundary layer and the quiescent nighttime atmosphere is clearly visible. (e) Vertical velocity skewness and boundary layer classification. Skewness of the velocity spectrum can be used to diagnose the source of turbulence (Hogan et al. 2009) and to classify different boundary layers types. Positive skewness (red) arises from surface-driven convection; negative skewness occurs at night, indicating convection driven by cooling at cloud top.

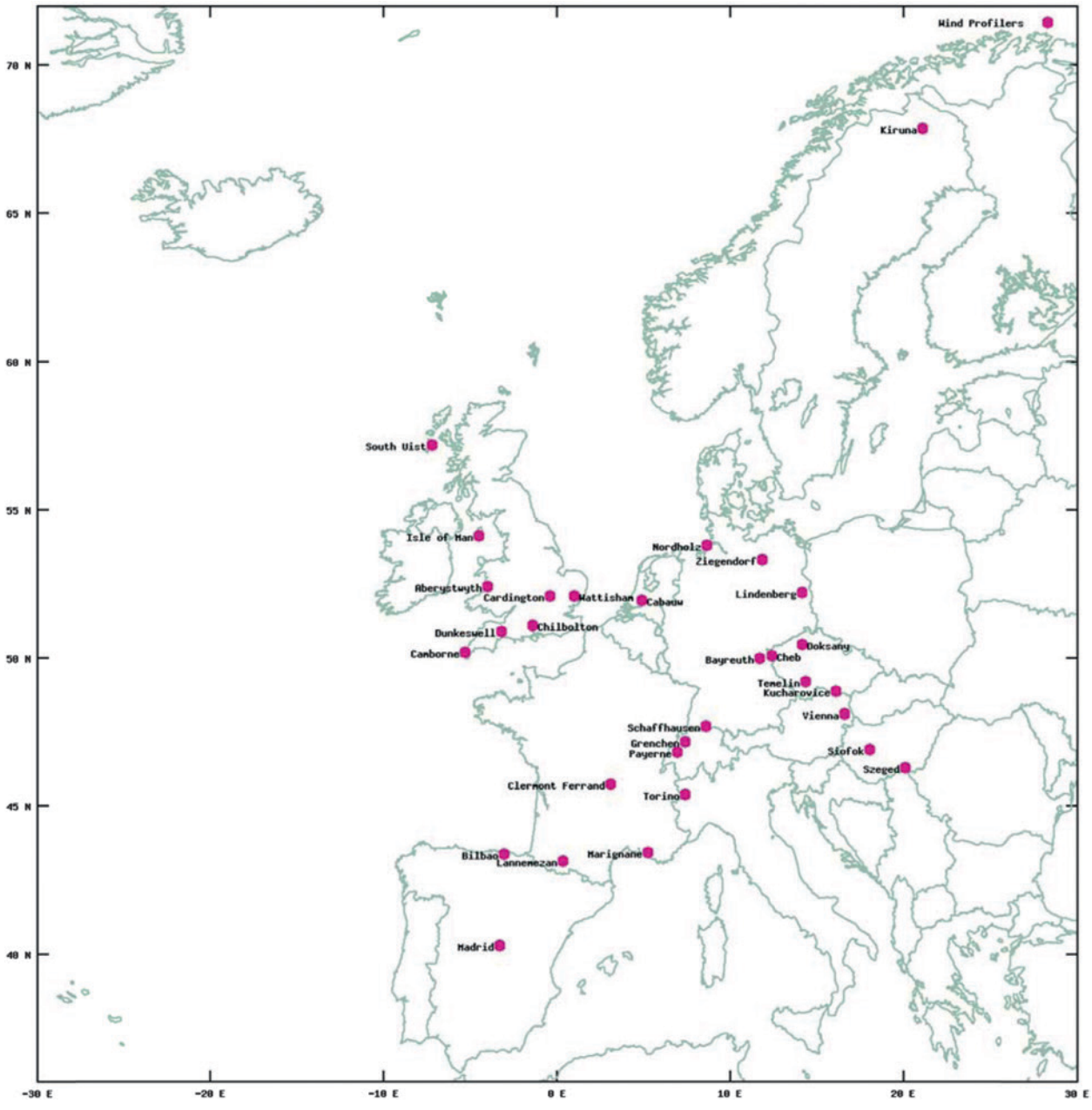

Fig. 7. Map showing the positions of the 30 WPs in the current European operational network.

convective motions. Barlow et al. (2011) discuss the use of a Doppler lidar to study boundary layer dynamics over London, United Kingdom. Dacre et al. (2010) report on the use of Doppler lidar to study the ash plume of the Icelandic volcano. Westbrook et al. (2010) describe how the properties of ice crystals falling from supercooled clouds can be inferred from Doppler lidar observations. Westbrook and Illingworth (2009) used Doppler lidar to infer the size spectrum of ice crystals in clouds.

Calibration and accuracy. The attenuated backscatter coefficient can be calibrated in the same way as ALCs (Westbrook et al. 2010). Doppler velocity is self-calibrating and biases can be diagnosed with tests using hard targets. The results for a comparison of winds derived from a Doppler lidar and a collocated wind profiler over several months at Lindenberg, Germany, show very low bias and rms errors. Details are in the next section on radar wind profilers.

The fiber-optic design allows for a high degree of flexibility, and these instruments are available in a number of guises with a multitude of possible measurement geometries, depending on the actual hardware: vertical stare only, full all-sky scanning capability, scan within a conical zone, or optimized

for winds only. Doppler lidar systems that specialize in vertical profiles of horizontal wind obtain this by means of "Doppler beam swinging," as is done for wind profilers, or through the use of a conical velocity–azimuth display (VAD) scan. Wind profiles are restricted to regions where there is sufficient aerosol to provide a good signal; in practice, this limits observations to within the boundary layer.

RADAR WIND PROFILERS. *Operational aspects.* Remote sensing of the horizontal wind vector in the atmosphere by a radar wind profiler (RWP) was demonstrated for the first time in the early 1970s (Woodman and Guillen 1974). Overviews of the technical and scientific aspects of RWPs have been provided by Gage (1990), Röttger and Larsen (1990), Doviak and Zrnić (1993), Muschinski (2004), and Fukao (2007). Quite a few operational networks worldwide provide continuous wind measurements in real time, and most of the data are successfully assimilated in numerical weather prediction models (Bouttier 2001; Benjamin et al. 2004; Ishihara et al. 2006; Calpini et al. 2011). In Europe, cooperative RWP networking began during the COST-76 action in early 1997 (Nash and Oakley 2001). The European network (Fig. 7) is currently run under the auspices of EUMETNET, with more than 25 instruments (June 2015).

The main advantage of RWPs is their ability to provide vertical profiles of the horizontal wind at high temporal resolution in both the cloudy and clear atmospheres. No other remote sensing method has this capability. The particular advantages of RWPs are a high temporal resolution and the provision of unambiguous profiles without additional a priori information. The majority of operationally used RWPs are monostatic pulse radars with a single (carrier) frequency (Muschinski et al. 2005). The wavelengths extend from about 20 cm (L band) to about 6 m [very high frequency (VHF)], so the scattering mechanism for "clear air" returns is the fluctuations of the refractive index on the scale of half the radar wavelength. The second major scattering process is due to cloud and precipitation particles, which are also assumed to be good tracers for the horizontal wind. All remaining echoes have to be treated as clutter, and their corresponding signal components need to be properly suppressed during signal processing. Of particular practical relevance are echoes from migrating birds (Wilczak et al. 1995). A novel filtering method based on a Gabor frame–based time–frequency decomposition of the raw data and signal statistics has been developed (Lehmann and Teschke 2008; Lehmann 2012) and has been successfully implemented in operational systems (Bianco et al. 2013).

For the retrieval of the wind vector, the (mean) wind field is assumed to be horizontally homogeneous over the sampled volume; therefore, averaging is performed for typically 10–60 min. Comparisons of RWP winds with data from a meteorological tower (Adachi et al. 2005) and balloon soundings (Rao et al. 2008) have shown that a four-beam-based Doppler beam swinging scanning configuration is superior to the minimum three-beam configuration in terms of data quality. The error of RWP wind measurements can be significantly reduced by increasing the number of off-vertical beams; Cheong et al. (2008) show that both five- and nine-beam configurations reduced the bias and variance resulting from deviations from the uniform wind field assumptions. As wind retrievals can be degraded during nonhomogeneous conditions—for example, in a convective boundary layer, during strong gravity wave activity (Weber et al. 1992), in patchy precipitation (Adachi et al. 2005), or in complex terrain (Bingöl et al. 2009)—additional quality control must be employed. Problems due to nonhomogeneous conditions have been noticed in NWP data assimilation (Cardinali 2009), but if more than three independent beam-pointing directions are used, then such cases can be identified by the inconsistency of the winds derived using different combinations of beams (e.g., Lau et al. 2013).

Accuracy and calibration. The precise estimation of Doppler frequencies is performed through heterodyning followed by spectral estimation methods and only requires sufficiently stable radio frequency (RF) oscillators. Precise ranging requires an accurate determination of the group delay of the signal in radar hardware that is easily achieved with standard test equipment. The accuracy of the wind measurement depends both on the correct estimation of the radial velocity in the radar resolution volume (which requires good clutter suppression) and the correct retrieval of the wind vector from the radial measurements (which requires homogeneity testing). The overall measurement quality is typically assessed through comparisons with wind measurements obtained with other upper-air wind measurements or NWP models. A recent intercomparison (Päschke et al. 2015) between a collocated 482-MHz RWP and a 1.5-μm Doppler lidar, based on more than 17,000 vertical wind profiles averaged over 30 min obtained over 12 months for the height range between 0.5 and 2.9 km, has shown a mean wind speed difference of less than 0.3 m s^{-1} and an RMS difference of less than

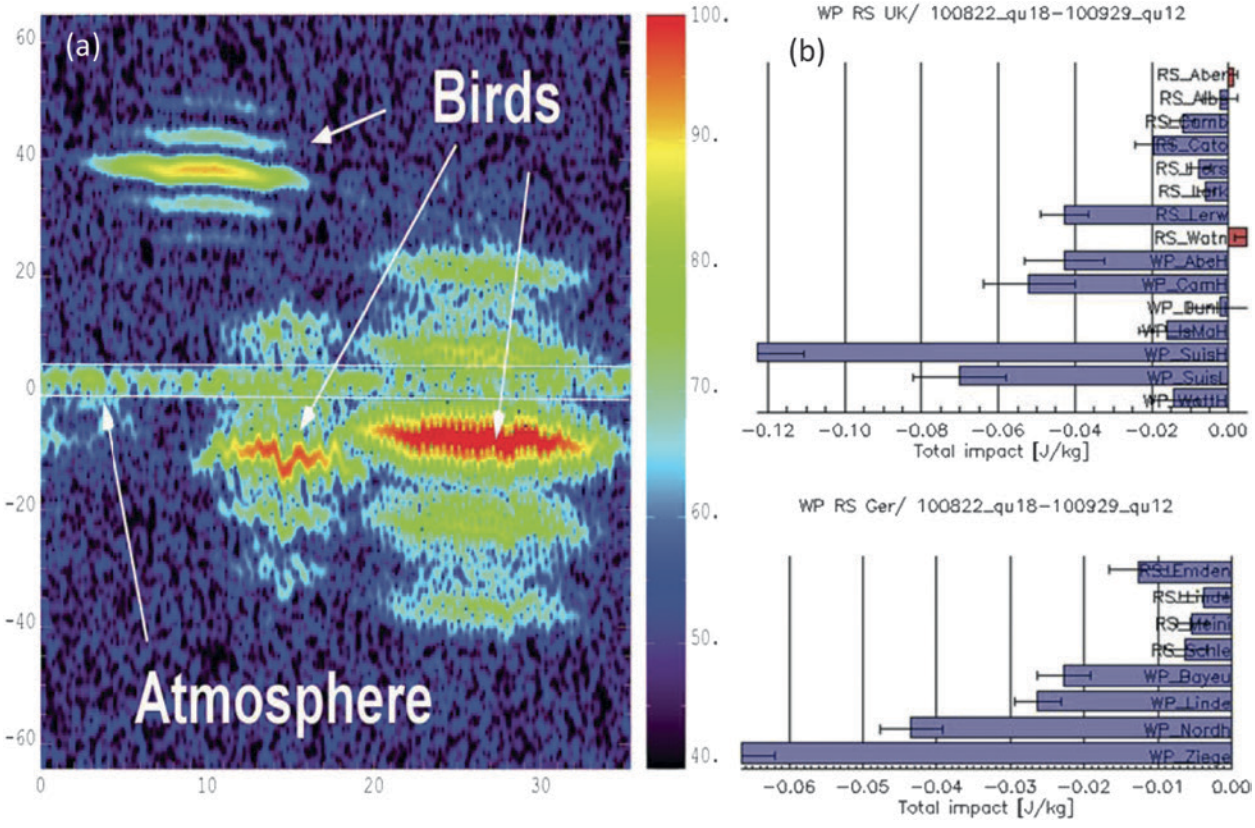

Fig. 8. New radar WP results. (a) Bird echo filtering. Time series of the power spectrum, where the abscissa shows time (s), the ordinate gives the frequency (Hz), and the color scale denotes signal power (dB). Two white lines at ±3 Hz define a clear distinction between the atmospheric returns and the higher-frequency returns due to the spurious returns from birds. (b) Larger positive impact of individual WPs on NWP forecasts when compared to the impact of individual RS for the (top) United Kingdom and (bottom) Germany to the reduction of forecast error analysis when assimilated into the MetOffice global NWP model. Errors are expressed in terms of the change in a global energy norm. Strategically placed profilers have a bigger impact than RS. (Courtesy of R. Leinweber, DWD, and C. Gaffard, MetOffice.)

0.7 m s^{-1}. A hardware issue affected the measurements below 1.2-km height, and when this was fixed, the bias was reduced to less than 0.1 m s^{-1}. The mean difference in wind direction was less than 1°, while the RMS difference was less than 10° over the whole height range. These errors are very low, so any comparison with radiosondes (RS) will be dominated by representativity errors. Because the lidar and profiler are making essentially point measurements, it is difficult to define a representativity error because this will depend upon the application, for example, the size of an NWP model grid box.

RWPs use sensitive low-noise amplifiers to detect extremely weak echoes. The availability of data under clear-air scattering conditions essentially depends on the variance spectrum of the refractive index at half the radar wavelength and is further a function of mean transmit power and antenna gain. The high sensitivity makes RWPs vulnerable to any external radio-frequency interference of sufficient strength that is in band. Frequency management is therefore an essential requirement for operational networks. RWPs require continuous data monitoring to identify malfunctions, and regular hardware maintenance is obviously a prerequisite for high data quality. However, commercial systems are quite mature and the required efforts are manageable with limited resources. A comprehensive discussion of various aspects of RWP maintenance can be found in Dibbern et al. (2001).

Impacts on numerical weather prediction. Two new results on radar wind profilers (RWPs) have been obtained during the EG-CLIMET project. First, a new method, now in operational use, has been developed (see Fig. 8a) that can identify and remove bird echoes; in the past returns from birds have resulted in spurious winds. Second, Fig. 8b displays the reduction of

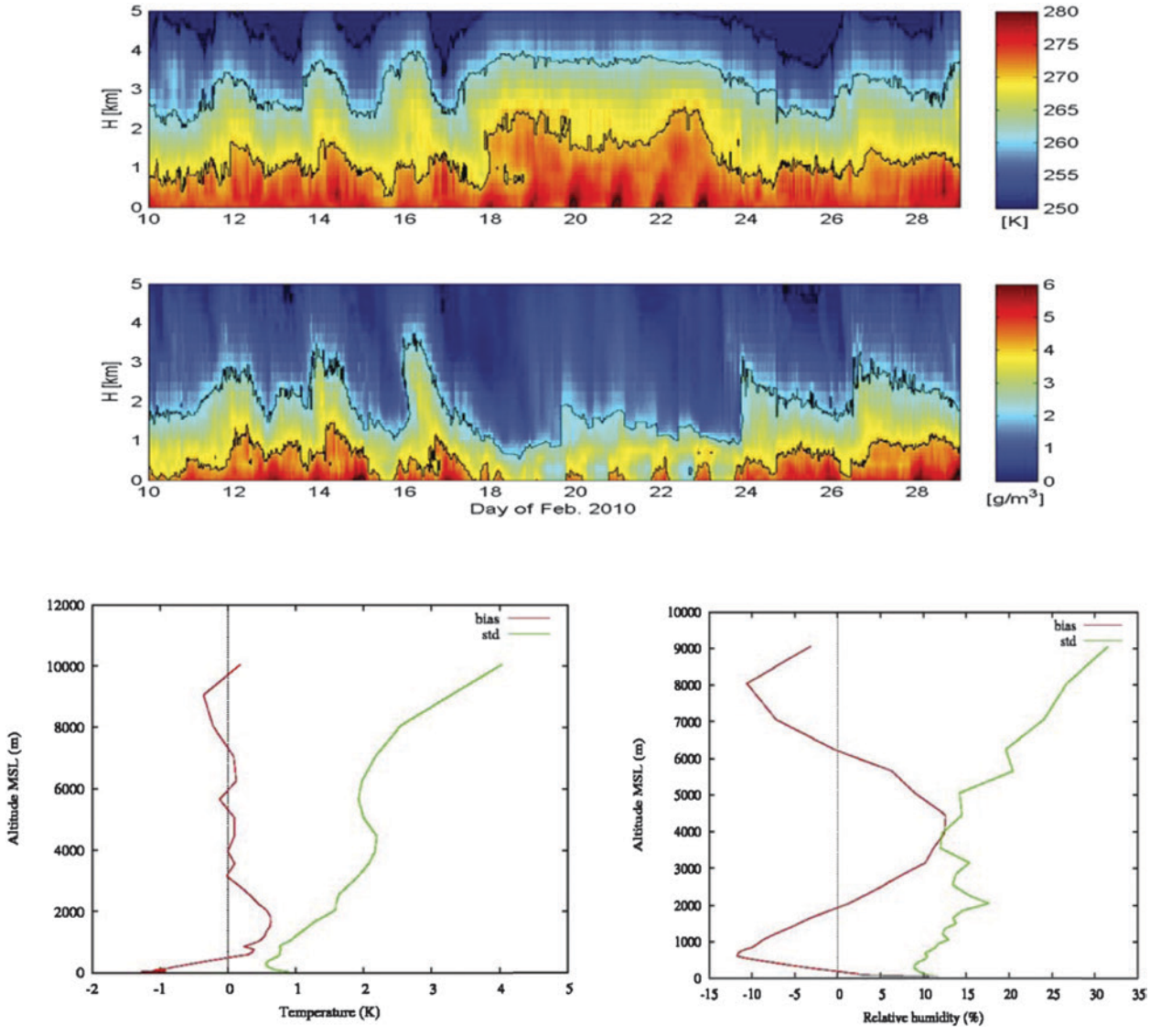

Fig. 9. (top),(middle) Temperature and water vapor density profiles over a 10-day period from a variational retrieval based on NWP profiles and multichannel MWR observations. (bottom) *O – B* statistics—that is, MWR-retrieved profiles minus NWP model [here, the French Applications of Research to Operations at Mesoscale (AROME) model], where mean (red) and standard deviation (green) differences—for (left) temperature and (right) relative humidity profiles from an MWR in Lampedusa, Italy (Cimini et al. 2014).

short-range forecast errors when observations from individual wind profilers are assimilated into NWP models using the forecast sensitivity to observation (FSO) method (Cardinali 2009; Lorenc and Marriott 2014). This relatively new technique makes it possible to compare the relative impact of different observing systems so, for the first time, the impact of each individual wind profiler can be objectively assessed. Figure 8b demonstrates that in both Germany and the United Kingdom, the cumulative impact of a well-maintained, continuously operating wind profiler can be many times that from the twice-daily ascents of a radiosonde. The greatest impacts were from isolated data-sparse sites, such as the profiler at South Uist in northwest Scotland and the Zeigendorf wind profiler in Germany. In contrast to this, in southern England many other observations are available and the profiler at Dunkerswell has a much smaller impact. This encouraging result highlights the potential of operational ground-based remote sensing of wind, especially if the profilers are strategically located in a data-sparse region.

MICROWAVE RADIOMETERS. Ground-based microwave radiometers (MWRs) measure the natural downwelling thermal emission in

the microwave part of the electromagnetic spectrum originating from Earth's atmosphere and from the cosmic background. The radiance observations are commonly expressed as an equivalent brightness temperature (Tb) from which estimates can be made of atmospheric temperature and humidity profiles and column-integrated water vapor (IWV) and liquid water path (LWP). Successful operational performance has been demonstrated (Güldner and Spänkuch 2001; Crewell and Löhnert 2003; Cimini et al. 2006). More recently, the benefits of MWR observations have also become clear during dynamic weather conditions (Knupp et al. 2009) and in support of nowcasting and short-range weather forecasting (Löhnert et al. 2007; Cimini et al. 2015). Figure 9 shows a 19-day time series of continuous temperature and humidity profiles under nearly all weather conditions obtained by applying a one-dimensional variational data assimilation (1D-VAR) retrieval framework (Cimini et al. 2011). Within EG-CLIMET, MWRs have also been used to successfully characterize the height of the atmospheric boundary layer within a multi-instrument comparison involving a ceilometer, Raman lidar, and radiosonde for NWP model evaluation as shown in Fig. 10 (Collaud Coen et al. 2014). The systems complement each other when the weather conditions allow planetary boundary layer (PBL) determination by one and not by another one (e.g., a ceilometer in case of clouds complemented by microwave radiometers). For this application, MWRs can provide an accurate and continuous addition to sparsely available radiosonde profiles (Cimini et al. 2013). Additionally, MWR data are used in a variety of other applications, including climate monitoring, studies on cloud microphysics, air quality prediction, satellite validation, radio astronomy, geodesy, air–sea interaction, and radio propagation.

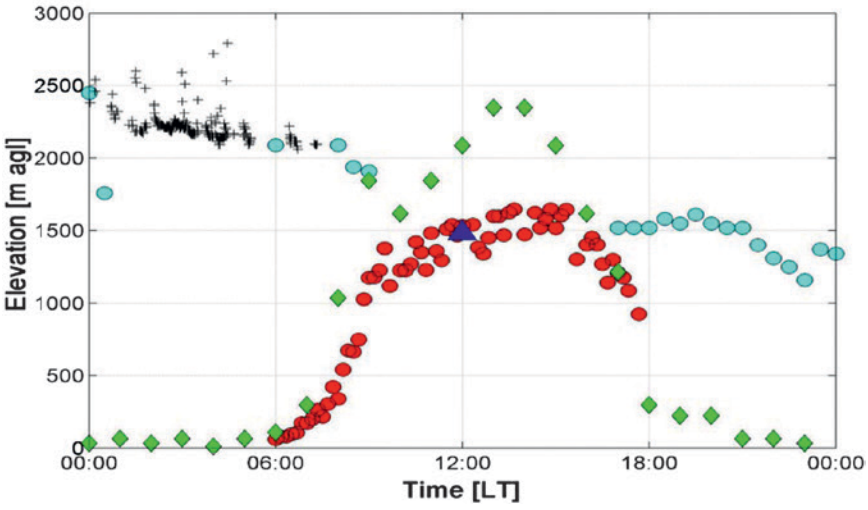

Fig. 10. Convective boundary layer heights over a 24-h period at Payerne, Switzerland, derived from different sources: MWR (red circles), RS (blue triangle), and DWD Consortium for Small-Scale Modeling (COSMO) NWP model (green diamonds). Light blue dots indicate the residual layer derived by Raman lidar; black crosses show ceilometer cloud base.

Operational aspects. Nowadays, off-the-shelf commercial MWRs consist of robust hardware exhibiting long life (years) even under extreme climatic conditions. The most common commercial units operate in the 20–60-GHz range. The 22–35-GHz band provides information on vapor and cloud liquid water due to the 22.235-GHz water vapor absorption line and the relative transparent atmospheric window at ~30 GHz. Two channels (usually 23.8 and 30–31 GHz) are required to retrieve IWV and LWP simultaneously. More channels provide information on the vertical distribution of water vapor content [WV(z)]. The 50–60-GHz band provides information on atmospheric temperature profiles $T(z)$, which are estimated from observations corresponding to varying opacity; this can be obtained either through single-channel observations at several elevation angles, through multichannel observations, or optimally through both (Crewell and Löhnert 2007). Applying automatic data quality and calibration control, MWRs can make high-quality continuous (time scales from seconds to minutes) observations of these thermodynamic atmospheric quantities in a long-term unattended mode under nearly all weather conditions.

Calibration and accuracy. Accurate MWR observations are subject to instrument integrity and proper signal calibration. Typically, MWRs are calibrated on the order of seconds to minutes using a blackbody target at ambient temperature and noise power sources. Parameters that are assumed stable within a calibration are determined through regular absolute calibrations every few months, applying either the so-called tipping curve method or a cryogenic external target. Manufacturers provide software and hardware tools

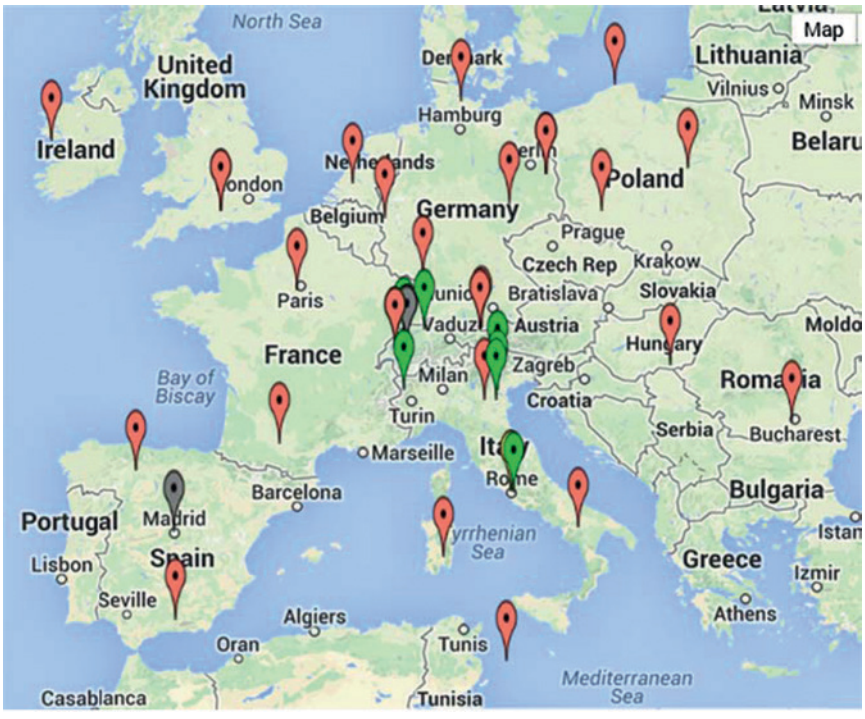

Fig. 11. MWRnet showing the sites over Europe. Different pin colors indicate different instruments: gray represents a generic system for propagation study; green represents a single-channel temperature (*T*) profiler; and red represents a multichannel *T* and water vapor (*V*) profiler.

to perform these methods though certain conditions (e.g., clear sky for tipping curve), and special care (e.g., liquid nitrogen for cryogenic) is required. When properly calibrated, an MWR provides Tb with an absolute accuracy of ~0.3–0.5 K (Maschwitz et al. 2013).

Considering the Tb accuracies and the ill-posed retrieval problem, typical resulting accuracies for derived atmospheric variables are as follows: IWV ~ 1.0 kg m^{-2}, LWP ~ 0.02 kg m^{-2}, $T(z)$ ~ 0.5–2.0 K, and WV(z) ~ 0.2–1.5 g m^{-3} (with the latter two decreasing from the surface upward). Löhnert et al. (2009) showed that for a generic MWR operating in the 20–60-GHz range, the number of independent levels that can be determined in the retrievals is approximately equal to two for humidity and four for temperature, where both these numbers depend on the moisture burden and the number of elevation angles. In particular, elevation scans are important for increasing the sensitivity to temperature inversions. Using scans at different elevations, MWRs are especially suited to accurately retrieve temperature inversions close to the surface, but they can also detect elevated inversions up to 1.5 km though with a smoothed inversion strength.

The accuracies given above exclude occasions when water accumulates over the radome, which represents a major limitation during precipitation. Mitigation solutions are used for current MWR instruments, including collocated rain sensor, hydrophobic coating, tangent blower, shutter, and side view. These effectively minimize the effect of dew and reduce water accumulation impacts on the retrieved products in most of the cases, with the exception of intense rainfall or snowfall. Generally, the radome protecting the antenna aperture must be kept clean, requiring regular services and replacement every few months depending upon environmental conditions (the presence of dirt, sand, and dust). Quality flags are usually adopted to indicate data during precipitation and/or with a wet radome.

Potential NWP impacts. The recent focus has been to demonstrate the data quality and the retrieval uncertainties for operational network application (Löhnert and Maier 2012; Güldner 2013) and to coordinate a network for the production of quality-controlled and harmonized data for the assimilation of MWR observations into NWP models (Cimini et al. 2014). For this, MWRnet—an international network of microwave radiometers (Fig. 11)—has been established within EG-CLIMET (http://cetemps.aquila.infn.it/mwrnet/). In addition to establishing protocols for harmonized network operation, first applications have been to create typical observation-minus-background statistics for a number of dedicated stations (Fig. 9, bottom). These encompass systematic and random differences of MWR temperature and humidity profile retrievals to the NWP background values and serve as quality control before the possible assimilation of these observations into NWP models. Preliminary results from the first data assimilation experiment of products generated by a continental-scale ground-based MWR network demonstrated that MWR data can be safely assimilated into NWP with a neutral-to-positive impact on forecasts' skills (Cimini et al. 2014).

SUMMARY OF FINDINGS AND RECOMMENDATIONS OF EG-CLIMET. EG-CLIMET has identified four classes of instruments—wind

profilers, automatic lidars and ceilometers (ALCs), Doppler lidars, and microwave radiometers—that are currently underexploited but could, with relatively low expenditure, make a significant contribution to NWP.

In earlier sections we have drawn attention to the following NWP applications of individual instruments and instruments in synergy:

- ALCs can be used for evaluation of NWP models' representation of clouds, aerosols, and mixing-layer heights, and potentially for data assimilation.
- Doppler lidars together with radar wind profilers can provide accurate winds throughout the troposphere.
- Strategically placed wind profilers have a positive impact on NWP forecasts.
- Radiosondes, microwave radiometers, ALCs, and Doppler lidars provide complementary views of the planetary boundary layer height, which can be used to evaluate NWP model–predicted boundary layer heights.
- The first analysis has been made of observations versus NWP model ($O - B$) statistics for temperature and relative humidity derived from a microwave radiometer.

An example of how observations from wind profilers and microwave radiometers can be used in an operational system to ensure a meteorological real-time surveillance in the case of nuclear hazard is given in Fig. 12 for a system that has been operational since 2009. Calpini et al. (2011) have demonstrated a positive impact of the three wind profilers on the quality of the forecast for the Swiss plateau.

Turning to the specific instruments:

For ALCs EG-CLIMET has

- demonstrated they could supply real-time backscatter profiles from clouds and aerosols;
- developed simple accurate calibration techniques using atmospheric targets;
- shown they can be used to infer the boundary layer height in unstable boundary layers; and
- made the first comparisons of the backscatter profiles of clouds and aerosols with NWP model predictions.

For Doppler lidars, EG-CLIMET has

- examined the performance of new Doppler lidars, 25 of which are now deployed in Europe;

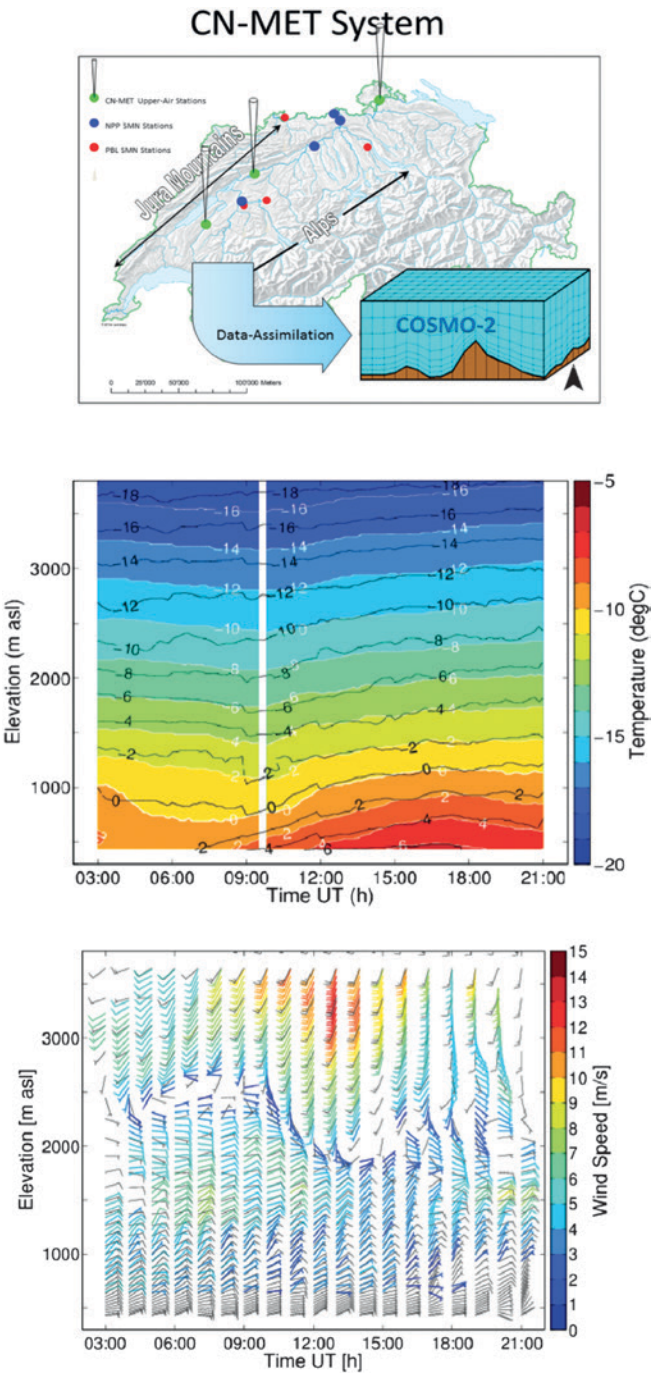

Fig. 12. Profilers for nuclear safety. Coupling of a specifically adapted measurement network (mainly WPs and MWRs) to a predictive tool (the COSMO-2 NWP model operated at MeteoSwiss to ensure a meteorological real-time surveillance in case of a nuclear hazard). (top) Illustration of the integrated online 24-h real-time system. (middle) Temperature profile time series from microwave radiometer (colored) overlaid with COSMO-2 isolines. (bottom) Wind speed and direction profiles from COSMO-2 (gray barbs) after assimilation of WP data (colored barbs). Calpini et al. (2011) have demonstrated a positive impact of the three WP on the quality of the forecast over the Swiss plateau. This system has been operational since 2009.

- demonstrated that they can provide accurate winds in the boundary layer; and
- shown that they can measure the height of the mixing layer, the decay of turbulent kinetic energy, the origin of vertical convective motions, and the vertical exchange in the boundary layer.

For radar wind profilers, EG-CLIMET has

- developed algorithms, now implemented operationally, to reject intermittent clutter echoes (e.g., birds);
- optimized algorithms for a better suppression of other spurious signals; and
- demonstrated the positive impact of well-maintained strategically placed wind profilers on NWP forecasts.

For microwave radiometers (MWRs), EG-CLIMET has

- compiled a list of MWRs in Europe and developed an international network: MWRnet;
- demonstrated the accuracy of temperature and water vapor in retrieved profiles;
- shown the value of MWR in estimating boundary layer depth; and
- provided the first comparisons of MWR retrievals with NWP model predictions.

What are the plans to exploit these instruments in an operational environment? The four instruments considered are at different states of maturity. The wind profilers are the most advanced, with a demonstrated positive impact on reducing forecast errors when assimilated into operational NWP models. The studies have also shown that it is essential that the profiler performance is monitored to ensure high data quality. EG-CLIMET has helped in defining and shaping the new E-PROFILE program set up by the Observations Program Manager Team ("Obs PMT") of EUMETNET, the body responsible for providing a framework for the European national weather services to work together. The E-PROFILE project (www.eumetnet.eu/e-profile), running from 2013 to 2017, is responsible for the management of the radar wind profiler network and for coordinating real-time exchange of backscatter profiles from ALCs.

Ceilometers have a long history as reliable all-weather instruments for monitoring the height of cloud base, and ALCs have now been established as also accurately measuring attenuated backscatter profiles of clouds and aerosols. E-PROFILE will coordinate the real-time exchange of data, but more work is needed on calibration and quality controlling the data for use in NWP. Doppler lidars show great promise, but again further studies are needed to evaluate their performance. For the microwave radiometers, much progress has been made establishing a global network. For all three instruments, further effort is required work to harmonize calibration routines, operating procedures, and retrieval algorithms so that the retrieved parameters can be compared with the values held in numerical weather prediction models; this will be followed by the first tests of the impact of assimilating the data. The new (2013–17) COST action ES1303 "Toward Operational Ground-Based Profiling with Ceilometers, Doppler Lidars and Microwave Radiometers for Improving Weather Forecasts" (TOPROF; www.toprof.eu) has been set up with the specific goal of addressing these issues for the three instruments. If these two projects—E-PROFILE and TOPROF—are successful, then we can expect that data from the various profilers discussed in this paper should be available in real time for use in NWP forecast models with a consequent potential improvement of their ability to predict hazardous weather events.

ACKNOWLEDGMENTS. The work described here was financed by the EU COST program (www.cost.eu).

REFERENCES

Adachi, A., T. Kobayashi, K. S. Gage, D. A. Carter, L. M. Hartten, W. L. Clark, and M. Fukuda, 2005: Evaluation of three-beam and four-beam profiler wind measurement techniques using a five-beam wind profiler and collocated meteorological tower. *J. Atmos. Oceanic Technol.*, **22**, 1167–1180, doi:10.1175/JTECH1777.1.

Barlow, J. F., T. M. Dunbar, E. G. Nemitz, C. R. Wood, M. W. Gallagher, F. Davies, E. O'Connor, and R. M. Harrison, 2011: Boundary layer dynamics over London, UK, as observed using Doppler lidar during REPARTEE-II. *Atmos. Chem. Phys.*, **11**, 2111–2125, doi:10.5194/acp-11-2111-2011.

Barrett, A. J., R. J. Hogan, and E. J. O'Connor, 2009: Evaluating forecasts of the evolution of the cloudy boundary layer using diurnal composites of radar and lidar observation. *Geophys. Res. Lett.*, **36**, L17811, doi:10.1029/2009GL038919.

Benjamin, S. G., B. E. Schwartz, S. E. Koch, and E. J. Szoke, 2004: The value of wind profiler in U.S. weather forecasting. *Bull. Amer. Meteor. Soc.*, **85**, 1871–1886, doi:10.1175/BAMS-85-12-1871.

Bianco, L., D. Gottas, and J. M. Wilczak, 2013: Implementation of a Gabor transform data quality-control algorithm for UHF wind profiling radars. *J. Atmos.*

Oceanic Technol., **30**, 2697–2703, doi:10.1175/JTECH-D-13-00089.1.

Bingöl, F., J. Mann, and D. Foussekis, 2009: Conically scanning lidar error in complex terrain. *Meteor. Z.*, **18**, 189–195, doi:10.1127/0941-2948/2009/0368.

Bouttier, F., 2001: The use of profiler data at ECMWF. *Meteor. Z.*, **10**, 497–510, doi:10.1127/0941-2948/2001/0010-0497.

Calpini, B., and Coauthors, 2011: Ground-based remote sensing profiling and numerical weather prediction model to manage nuclear power plants meteorological surveillance in Switzerland. *Atmos. Meas. Tech.*, **4**, 1617–1625, doi:10.5194/amt-4-1617-2011.

Cardinali, C., 2009: Monitoring the observation impact on the short-range forecast. *Quart. J. Roy. Meteor. Soc.*, **135**, 239–250, doi:10.1002/qj.366.

Cheong, B. L., R. D. Palmer, T-Y. Yu, K-F. Yang, M. W. Hoffman, S. J. Frasier, and F. J. Lopez-Dekker, 2008: Effects of wind field inhomogeneities on Doppler beam swinging revealed by an imaging radar. *J. Atmos. Oceanic Technol.*, **25**, 1414–1422, doi:10.1175/2007JTECHA969.1.

Cimini, D., T. J. Hewison, L. Martin, J. Güldner, C. Gaffard, and F. S. Marzano, 2006: Temperature and humidity profile retrievals from ground-based microwave radiometers during TUC. *Meteor. Z.*, **15**, 45–56, doi:10.1127/0941-2948/2006/0099.

——, and Coauthors, 2011: Thermodynamic atmospheric profiling during the 2010 Winter Olympics using ground-based microwave radiometry. *IEEE Trans. Geosci. Remote Sens.*, **49**, 4959–4969, doi:10.1109/TGRS.2011.2154337.

——, F. De Angelis, J.-C. Dupont, S. Pal, and M. Haeffelin, 2013: Mixing layer height retrievals by multichannel microwave radiometer observations. *Atmos. Meas. Tech.*, **6**, 2941–2951, doi:10.5194/amt-6-2941-2013.

——, and Coauthors, 2014: A data assimilation experiment of temperature and humidity profiles from an international network of ground-based microwave radiometers. *MicroRad 2014: 13th Specialist Meeting on Microwave Radiometry and Remote Sensing of the Environment*, Pasadena, CA, IEEE, 81–84.

——, M. Nelson, J. Güldner, and R. Ware, 2015: Forecast indices from ground-based microwave radiometer for operational meteorology. *Atmos. Meas. Tech.*, **8**, 315–333, doi:10.5194/amt-8-315-2015.

Collaud Coen, M., C. Praz, A. Haefele, D. Ruffieux, P. Kaufmann, and B. Calpini, 2014: Determination and climatology of the planetary boundary layer height by in-situ and remote sensing methods as well as the COSMO model above the Swiss plateau. *Atmos. Chem. Phys. Discuss.*, **14**, 15 419–15 462, doi:10.5194/acpd-14-15419-2014.

COST, 2013: COST Action ES0702 EG-CLIMET—Final report. COST Rep. PUB1062, date accessed 1 Feb 2015. [Available online at http://cfa.aquila.infn.it/wiki.eg-climet.org/index.php5/Final_Report.]

Crewell, S., and U. Löhnert, 2003: Accuracy of cloud liquid water path from ground-based microwave radiometry. 2. Sensor accuracy and synergy. *Radio Sci.*, **38**, 8042, doi:10.1029/2002RS002634.

——, and ——, 2007: Accuracy of boundary layer temperature profiles retrieved with multi-frequency, multi-angle microwave radiometry. *IEEE Trans. Geosci. Remote Sens.*, **45**, 2195–2201, doi:10.1109/TGRS.2006.888434.

Dacre, H., and Coauthors, 2010: Evaluating the structure and magnitude of the ash plume during the initial phase of the 2010 Eyjafjallajökull eruption using lidar observations and NAME simulations. *J. Geophys. Res.*, **116**, D00U03, doi:10.1029/2011JD015608.

Dibbern, J., W. Monna, J. Nash, and G. Peters, Eds., 2001: Development of VHF/UHF wind profilers and vertical sounders for use in European observing systems. Final Rep., COST Action 76, European Commission, 350 pp.

Doviak, R. J., and D. S. Zrnić, 1993: *Doppler Radar and Weather Observations*. Academic Press, 562 pp.

Emeis, S., K. Schäfer, and C. Münkel, 2008: Surface-based remote sensing of the mixing-layer height: A review. *Meteor. Z.*, **17**, 621–630, doi:10.1127/0941-2948/2008/0312.

Flentje, H., and Coauthors, 2010: The Eyjafjallajökull eruption in 2010—Detection of volcanic plume using in-situ measurements, ozone sondes and lidar-ceilometer profiles. *Atmos. Chem. Phys.*, **10**, 10 085–10 092, doi:10.5194/acp-10-10085-2010.

Fukao, S., 2007: Recent advances in atmospheric radar study. *J. Meteor. Soc. Japan*, **85B**, 215–239, doi:10.2151/jmsj.85B.215.

Gage, K. S., 1990: Radar observations of the free atmosphere: Structure and dynamics. *Radar in Meteorology*, D. Atlas, Ed., Amer. Meteor. Soc., 534–565.

Güldner, J., 2013: A model-based approach to adjust microwave observations for operational applications: Results of a campaign at Munich Airport in winter 2011/2012. *Atmos. Meas. Tech. Discuss.*, **6**, 2935–2954, doi:10.5194/amtd-6-2935-2013.

——, and D. Spänkuch, 2001: Remote sensing of the thermodynamic state of the atmospheric boundary layer by ground-based microwave radiometry. *J. Atmos. Oceanic Technol.*, **18**, 925–933, doi:10.1175/1520-0426(2001)018<0925:RSOTTS>2.0.CO;2.

Haeffelin, M., and Coauthors, 2012: Evaluation of mixing height retrievals from automatic profiling lidars and ceilometers in view of future integrated

networks in Europe. *Bound.-Layer Meteor.*, **143**, 49–75, doi:10.1007/s10546-011-9643-z.

Hogan, R. J., A. L. M. Grant, A. J. Illingworth, G. N. Pearson, and E. J. O'Connor, 2009: Vertical velocity variance and skewness in clear and cloud-topped boundary layers as revealed by Doppler lidar. *Quart. J. Roy. Meteor. Soc.*, **135**, 635–643, doi:10.1002/qj.413.

Illingworth, A. J., and Coauthors, 2007: Cloudnet: Continuous evaluation of cloud profiles in seven operational models using ground-based observations. *Bull. Amer. Meteor. Soc.*, **88**, 883–898, doi:10.1175/BAMS-88-6-883.

——, D. Ruffieux, D. Cimini, U. Löhnert, M. Haeffelin, and V. Lehmann, Eds, 2013: COST Action ES0702 EG-CLIMET——Final report. COST Rep. PUB1062, 141 pp., doi:10.12898/ES0702FR.

Ishihara, M., Y. Kato, T. Abo, K. Kobayashi, and Y. Izumikawa, 2006: Characteristics and performance of the operational wind profiler network of the Japan Meteorological Agency. *J. Meteor. Soc. Japan*, **84**, 1085–1096, doi:10.2151/jmsj.84.1085.

Klett, J. D., 1981: Stable analytical inversion solution for processing lidar returns. *Appl. Opt.*, **20**, 211–220, doi:10.1364/AO.20.000211.

Knupp, K. R., R. Ware, D. Cimini, F. Vandenberghe, J. Vivekanandan, E. Westwater, T. Coleman, and D. Phillips, 2009: Ground-based passive microwave profiling during dynamic weather conditions. *J. Atmos. Oceanic Technol.*, **26**, 1057–1073, doi:10.1175/2008JTECHA1150.1.

Lau, E., and Coauthors, 2013: The DeTect Inc. RAPTOR VAD-BL radar wind profiler. *J. Atmos. Oceanic Technol.*, **30**, 1978–1984, doi:10.1175/JTECH-D-12-00259.1.

Lehmann, V., 2012: Optimal Gabor-frame-expansion-based intermittent-clutter-filtering method for radar wind profiler. *J. Atmos. Oceanic Technol.*, **29**, 141–158, doi:10.1175/2011JTECHA1460.1.

——, and G. Teschke, 2008: Advanced intermittent clutter filtering for radar wind profiler: Signal separation through a Gabor frame expansion and its statistics. *Ann. Geophys.*, **26**, 759–783, doi:10.5194/angeo-26-759-2008.

Löhnert, U., and O. Maier, 2012: Operational profiling of temperature using ground-based microwave radiometry at Payerne: Prospects and challenges. *Atmos. Meas. Tech.*, **5**, 1121–1134, doi:10.5194/amt-5-1121-2012.

——, E. van Meijgaard, H. K. Baltink, S. Groß, and R. Boers, 2007: Accuracy assessment of an integrated profiling technique for operationally deriving profiles of temperature, humidity and cloud liquid water. *J. Geophys. Res.*, **112**, D04205, doi:10.1029/2006JD007379.

——, D. D. Turner, and S. Crewell, 2009: Ground-based temperature and humidity profiling using spectral infrared and microwave observations. Part I: Simulated retrieval performance in clear-sky conditions. *J. Appl. Meteor. Climatol.*, **48**, 1017–1032, doi:10.1175/2008JAMC2060.1.

Lorenc, A. C., and R. T. Marriott, 2014: Forecast sensitivity to observations in the Met Office global numerical weather prediction system. *Quart. J. Roy. Meteor. Soc.*, **140**, 209–224, doi:10.1002/qj.2122.

Maschwitz, G., U. Löhnert, S. Crewell, T. Rose, and D. D. Turner, 2013: Investigation of ground-based microwave radiometer calibration techniques at 530 hPa. *Atmos. Meas. Tech. Discuss.*, **6**, 989–1032, doi:10.5194/amtd-6-989-2013.

Morille, Y., M. Haeffelin, P. Drobinski, and J. Pelon, 2007: STRAT: An automated algorithm to retrieve the vertical structure of the atmosphere from single-channel lidar data. *J. Atmos. Oceanic Technol.*, **24**, 761–775, doi:10.1175/JTECH2008.1.

Münkel, C., N. Eresmaa, J. Räsänen, and A. Karppinen, 2007: Retrieval of mixing height and dust concentration with lidar ceilometer. *Bound.-Layer Meteor.*, **124**, 117–128, doi:10.1007/s10546-006-9103-3.

Muschinski, A., 2004: Local and global statistics of clear-air Doppler radar signals. *Radio Sci.*, **39**, RS1008, doi:10.1029/2003RS002908.

——, V. Lehmann, L. Justen, and G. Teschke, 2005: Advanced radar wind profiling. *Meteor. Z.*, **14**, 609–626, doi:10.1127/0941-2948/2005/0067.

Nash, J., and T. J. Oakley, 2001: Development of COST 76 wind profiler network in Europe. *Phys. Chem. Earth*, **26B**, 193–199, doi:10.1016/S1464-1909(00)00239-2.

NRC, 2009: *Observing Weather and Climate from the Ground Up: A Nationwide Network of Networks*. National Academies Press, 250 pp.

——, 2010: *When Weather Matters: Science and Service to Meet Critical Societal Needs.* National Academies Press, 198 pp.

O'Connor, E. J., A. J. Illingworth, and R. J. Hogan, 2004: A technique for autocalibration of cloud lidar. *J. Atmos. Oceanic Technol.*, **21**, 777–786, doi:10.1175/1520-0426(2004)021<0777:ATFAOC>2.0.CO;2.

——, ——, I. M. Brooks, C. D. Westbrook, R. J. Hogan, F. Davies, and B. J. Brooks, 2010: A method for estimating the turbulent kinetic energy dissipation rate from a vertically pointing Doppler lidar, and independent evaluation from balloon-borne in-situ measurements. *J. Atmos. Oceanic Technol.*, **27**, 1652–1664, doi:10.1175/2010JTECHA1455.1.

Pal, S., M. Haeffelin, and E. Batchvarova, 2013: Exploring a geophysical process-based attribution technique for the determination of the atmospheric

boundary layer depth using aerosol lidar and near-surface meteorological measurements. *J. Geophys. Res. Atmos.*, **118**, 9277–9295, doi:10.1002/jgrd.50710.

Päschke, E., R. Leinweber, and V. Lehmann, 2015: A one year comparison of 482 MHz radar wind profiler, RS92-SGP Radiosonde and 1.5 μm Doppler lidar wind measurements. *Atmos. Meas. Tech.*, **8**, 2251–2266, doi:10.5194/amt-8-2251-2015.

Rao, I. S., V. K. Anandan, and P. N. Reddy, 2008: Evaluation of DBS wind measurement technique in different beam configurations for a VHF wind profiler. *J. Atmos. Oceanic Technol.*, **25**, 2304–2312, doi:10.1175/2008JTECHA1113.1.

Röttger, J., and M. F. Larsen, 1990: UHF/VHF radar techniques for atmospheric research and wind profiler applications. *Radar in Meteorology*, D. Atlas, Ed., Amer. Meteor. Soc., 235–281.

Weber, B. L., D. B. Wuertz, D. C. Law, A. S. Frisch, and J. M. Brown, 1992: Effects of small/scale vertical motion on radar measurements of wind and temperature profiles. *J. Atmos. Oceanic Technol.*, **9**, 193–209, doi:10.1175/1520-0426(1992)009<0193:EOSSVM>2.0.CO;2.

Westbrook, C. D., and A. J. Illingworth, 2009: Testing the influence of small crystals on ice size spectra using Doppler lidar observations. *Geophys. Res. Lett.*, **36**, L12810, doi:10.1029/2009GL038186.

——, ——, E. J. O'Connor, and R. J. Hogan, 2010: Doppler lidar measurements of oriented planar ice crystals falling from supercooled and glaciated cloud layers. *Quart. J. Roy. Meteor. Soc.*, **136**, 260–276, doi:10.1002/qj.528.

Wiegner, M., and A. Geiß, 2012: Aerosol profiling with the Jenoptik ceilometer CHM15kx. *Atmos. Meas. Tech.*, **5**, 1953–1964, doi:10.5194/amt-5-1953-2012.

Wilczak, J., and Coauthors, 1995: Contamination of wind profiler data by migrating birds: Characteristics of corrupted data and potential solutions. *J. Atmos. Oceanic Technol.*, **12**, 449–467, doi:10.1175/1520-0426(1995)012<0449:COWPDB>2.0.CO;2.

WMO, 2014: Statement of guidance for global numerical weather prediction (NWP). 10 pp. [Available online at www.wmo.int/pages/prog/www/OSY/SOG/SoG-Global-NWP.pdf.]

Woodman, R. F., and A. Guillen, 1974: Radar observation of winds and turbulence in the stratosphere and mesosphere. *J. Atmos. Sci.*, **31**, 493–505, doi:10.1175/1520-0469(1974)031<0493:ROOWAT>2.0.CO;2.

Science at Your Fingertips

AMS Journals are now optimized for viewing on your mobile device.

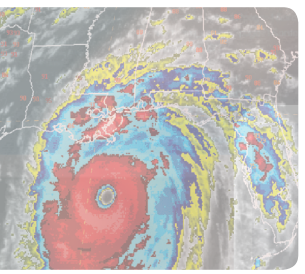

Access journal articles, monograph titles, and BAMS content using your iOS, Android, or Blackberry phone, or tablet.

Features include:

- **Saving articles for offline reading**
- **Sharing of article links via email and social networks**
- **Searching across journals, authors, and keywords**

And much more...

Scan code to connect to journals.ametsoc.org

AMERICAN METEOROLOGICAL SOCIETY